

Article

Migration and Transformation of Nitrogen in Clay-Rich Soil Under Shallow Groundwater Depth: In Situ Experiment and Numerical Simulation

Jinting Huang ^{1,*}, Qiu Lv ¹, Zhan Yang ¹, Fang Pu ¹, Ge Song ¹, Jiawei Wang ¹, Zongze Li ¹, Tuo Fang ¹, Tian Huang ¹, Fang Zhang ² and Fangqiang Sun ²

¹ Geology and Environment College, Xi'an University of Science and Technology, Xi'an 710054, China; 22209226045@stu.xust.edu.cn (Q.L.); 17729381671@163.com (Z.Y.); pufang@163.com (F.P.); 20209226102@xust.edu.cn (G.S.); wangjw7659@163.com (J.W.); 2023029012@chd.edu.cn (Z.L.); 18292856580@163.com (T.F.); h17381253885@163.com (T.H.)

² Xi'an Center of Geological Survey (CGS), Xi'an 710054, China; zhangfanghz@163.com (F.Z.); sunfq2003@126.com (F.S.)

* Correspondence: hjinting@xust.edu.cn; Tel.: +86-13572521980

Abstract: Excessive use of nitrogen fertilizer in agricultural activities can easily induce nitrogen pollution in groundwater, which may deteriorate groundwater quality. Generally, nitrogen fertilizer passes through the unsaturated zone to groundwater. Therefore, it is of great significance to investigate the migration and transformation of nitrogen pollutants in unsaturated zones for the prevention and control of groundwater nitrogen pollution. Clay-rich soil is often considered a barrier layer to prevent pollutant leakage because of its lower relative permeability, while its prevention capacity is seldom reported under shallow groundwater table conditions. Motivated by this, an in situ experiment and numerical simulation were conducted to investigate the migration and transformation of nitrogen fertilizer in a clay-unsaturated zone with a shallow groundwater table. Systematic measurements and numerical simulation results revealed that nitrogen can pollute groundwater via the infiltration through clay-rich soil in the in situ experiment site. This finding clarified that the difference in hydraulic head under the shallow groundwater table, rather than soil permeability, is the dominant factor in controlling the downward migration of nitrogen pollutants in the clay-unsaturated zone. More importantly, the nitrogen migration is convection dominant during precipitation in this experiment, indicating nitrogen polluted groundwater much faster in humid climate areas. These findings suggest that nitrogen contaminates groundwater easily under shallow groundwater tables in humid climate areas, even with clay-rich soil texture.

Keywords: in situ experiment; HYDRUS-1D; shallow groundwater table; nitrogen pollutant; clay-unsaturated zone; Hanzhong Basin



Academic Editors: Maurizio Barbieri and Craig Allan

Received: 15 October 2024

Revised: 28 January 2025

Accepted: 30 January 2025

Published: 3 February 2025

Citation: Huang, J.; Lv, Q.; Yang, Z.; Pu, F.; Song, G.; Wang, J.; Li, Z.; Fang, T.; Huang, T.; Zhang, F.; et al.

Migration and Transformation of Nitrogen in Clay-Rich Soil Under Shallow Groundwater Depth: In Situ Experiment and Numerical Simulation. *Water* **2025**, *17*, 427. <https://doi.org/10.3390/w17030427>

Copyright: © 2025 by the authors. Licensee MDPI, Basel, Switzerland. This article is an open access article distributed under the terms and conditions of the Creative Commons Attribution (CC BY) license (<https://creativecommons.org/licenses/by/4.0/>).

1. Introduction

In recent decades, the application of large amounts of nitrogen fertilizers in croplands around the world has led to severe excesses of ammonia in groundwater [1–3]. The migration and transformation of nitrogen in the vadose zone are influenced by many factors, such as soil physicochemical properties, soil nitrogen composition, fertilization, precipitation, and irrigation [4,5]. Among these factors, precipitation and soil water dynamics strongly regulate the nitrogen cycle by affecting the migration and distribution characteristics of ni-

trogen in the vadose zone [6,7]. Thus, one of the scientific challenges is to quantify the effect of multi-factors on the migration of nitrogen under changing environmental conditions.

Due to the highly nonlinear migration and transformation of nitrogen in the unsaturated zone and the complexity of chemical reactions, many efforts have been expended on the nitrogen pollution mechanisms, physical and chemical properties of the unsaturated zone, and irrigation intensity [8–10]. In previous research, environmental factors and human activities were the predominant factors in terms of nitrogen migration and transformation. The environmental factors include precipitation, pH, soil redox environment, soil moisture, organic carbon content, available oxygen content, groundwater depth, and unsaturated lithology structure [11–14]. The effects of human activities refer to crop species, different planting methods, fertilization, irrigation amount, and irrigation methods [15–20]. Already published research results show that precipitation, irrigation amount and method, lithology structure of unsaturated zone, and groundwater depth indirectly affect the migration and transformation of nitrogen pollutants through soil moisture content and oxygen levels. Clay-rich soil is often applied as a barrier layer to block nitrogen pollution since nitrogen migration and transformation are faster in coarse soil [21–23]. Previous work has studied the migration and transformation of nitrogen in a laboratory-scale soil column experiment, which had important guiding significance for the prevention and control of groundwater pollution [24,25]. Meanwhile, groundwater depth also affects the migration and transformation of nitrogen since nitrogen species are more likely to reach groundwater when the groundwater depth is shallow [26,27]. Therefore, more work on the co-effects of clay-rich soil and shallow groundwater depth on nitrogen migration and transformation is needed to improve the understanding of the domination processes and controls for changing environmental variables.

Numerical models are commonly used to quantify the migration and transformation of nitrogen in saturated and unsaturated zones. Previous studies have explored the forms and pollution of nitrogen in unsaturated zones by establishing mathematical models solely or combining them with laboratory-scale soil column experiments. These numerical models involve the absorption and rate of nitrogen in ponding, nitrogen migration, or nitrogen cycle in soil [28–37]. It has been found that the main forms of nitrogen in the soil are ammonia nitrogen ($\text{NH}_4^+\text{-N}$) and nitrate nitrogen ($\text{NO}_3^-\text{-N}$). The adsorption of $\text{NH}_4^+\text{-N}$ by soil is greater than that of $\text{NO}_3^-\text{-N}$, and the pollution form of nitrogen in groundwater is mainly nitrate [38,39]. In terms of the influence of unsaturated zone thickness and permeability on nitrogen migration and transformation, it was found that groundwater had a high risk of nitrogen pollution in the thin vadose zone with high permeability [40], while nitrogen pollution rarely occurred in the area where the groundwater was buried deeper than 10 m and unsaturated zone has low permeability. Controlling irrigation intensity can also effectively reduce groundwater nitrogen pollution. The working hypothesis of this study is that the unique hydrogeological conditions of shallow groundwater tables significantly influence the process of nitrogen migration and transformation, thereby increasing the risk of groundwater contamination in clay-rich soil under humid climates. Based on this hypothesis, we conducted field experiments and numerical simulations to delve into the migration and transformation patterns of nitrogen fertilizers under shallow groundwater table conditions in the clay-unsaturated zone. Specifically, this study aims to address the following question: How do shallow groundwater tables in the clay-unsaturated zones synergistically affect the migration and transformation of nitrogen contaminants? The elucidation of this process is crucial for understanding and predicting the risk of groundwater nitrogen contamination in humid climates. This research holds significant importance for the formulation of effective strategies to prevent and control groundwater contamination.

2. Materials and Methods

2.1. Field Experiment and Measurements

2.1.1. Site Description

The in situ experiment for the investigation of nitrogen migration and transformation was carried out in the farmland of Wangzhuang Village, Wuxiang Township, Hantai District, Hanzhong City, Shaanxi Province, China (107°1' E, 33°12' N, altitude 632.5 m, Figure 1). This region belongs to a subtropical humid monsoon climate. Annual average temperature is 14.5 °C. Annual average precipitation is 855.3 mm, and precipitation is mainly concentrated in June to September. The average relative humidity is 79%. The annual average sunshine hours is 1478.4 h. Annual total radiation is 105.1 Kcal/cm². This experimental field is a gentle slope terraced field. The crops are corn, rape, and seasonal vegetables. The texture of the unsaturated zone is silt clay according to soil particle analysis (Table 1).

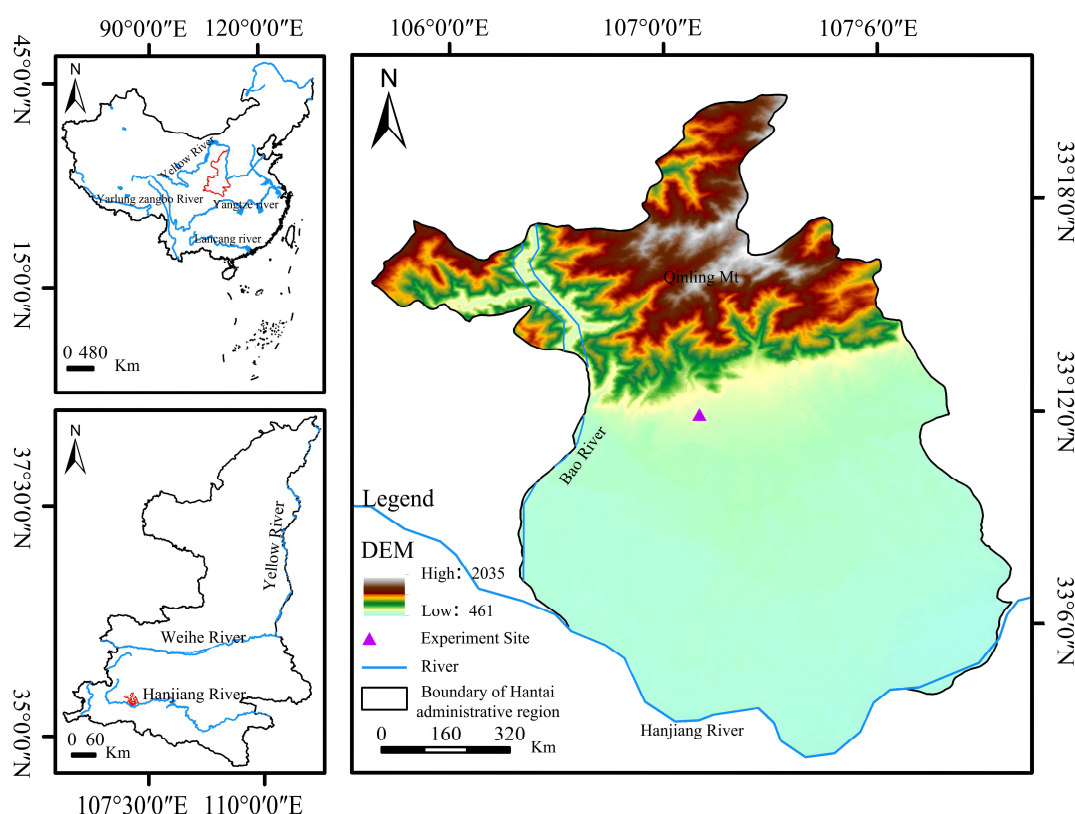


Figure 1. Location of the in situ experiment.

Table 1. Soil texture and bulk density at different depths at the in situ site.

Depth (cm)	Soil Particle Size Distribution			Texture	Bulk Density (g/cm ³)
	Sand (%)	Silt (%)	Clay (%)		
0–10	2.2	68.1	29.7	silt clay	1.50
10–20	1.7	61.7	36.6	silt clay	1.65
20–40	1.7	56.6	41.7	silt clay	1.60
40–60	0.0	58.7	41.3	silt clay	1.76
60–80	0.0	55.2	44.8	silt clay	1.68
80–100	0.0	56.6	43.4	silt clay	1.63
100–120	0.0	54.2	45.8	silt clay	1.70
120–140	0.9	60.2	38.9	silt clay	1.50
140–155	1.5	59.1	39.4	silt clay	1.35
155–175	2.3	57.4	40.3	silt clay	1.35

2.1.2. Instrument Set-Up

This research site consists of an area of 30 m × 30 m. The in situ experiment site consists of 4 parts, including a spray infiltration area, soil water content measurement, soil nitrogen concentration samples collection shaft, meteorological variables monitoring area, groundwater level, and groundwater quality monitoring wells (Figure 2). The spray area is 2 m in length and 1.5 m in width. Nitrogen solute with pressureless spray was used to simulate the infiltration of nitrogen pollutants under precipitation recharge. A spray frame with spray sensors was installed 80 cm high above the ground surface. Nitrogen solute supplied by a peristaltic pump ensures a foggy spray solution with no pressure on the ground surface. A shaft with 1.5 m length, 1.2 m width, and 1.8 m depth was dug for soil water content measurement and soil nitrogen sample collection 0.3 m distant from the spraying area. A set of instruments was installed to measure soil water contents, soil matrix potentials, groundwater levels, and meteorological variables. Soil water content sensors (EC-5, Meter Inc., Pullman, WA, USA) were installed in the shaft at the depths of 10, 20, 40, 60, 80, 100, 120, 140, and 155 cm. All data were collected by a data logger (CR3000, Campbell Scientific, Logan, UT, USA) every 60 s, and 10-min averages were calculated and stored. A data logger (Rugged Troll 100, In situ Inc. Fort Collins, CO, USA) was installed in a piezometer (at a 400 cm depth below the ground surface) to monitor the groundwater level and temperature. The piezometer was covered by a ventilated PVC cap for protection. The data were recorded at 10 s intervals and stored as 10 min average values. A tintage meteorological station, Vantage Pro2 (DAVIS Inc., Hayward, CA, USA), was installed at the research plot 2 m above the ground surface to measure wind speed and direction, air temperature and humidity, solar radiation, rainfall, and air pressure.

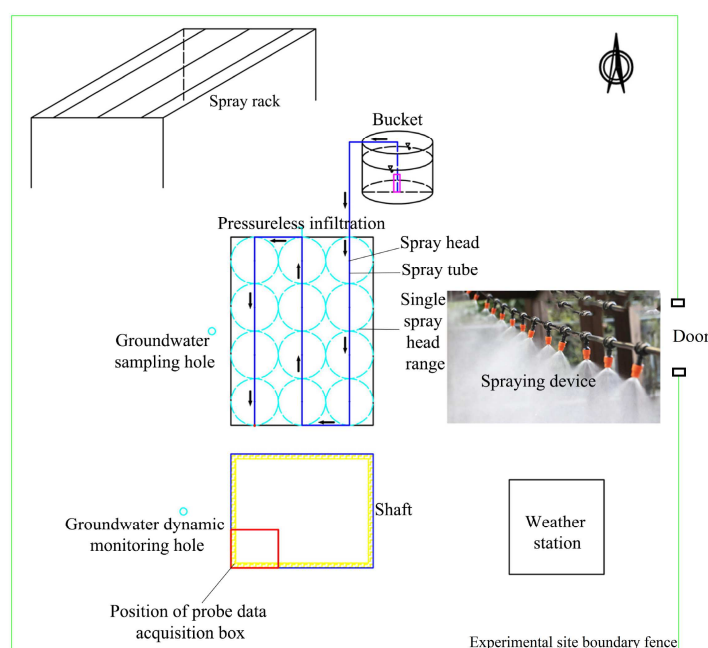


Figure 2. Layout of the in situ experiment site.

2.1.3. Sample Collection and Analysis

Soil samples were collected during the shaft dig for soil background nitrogen analysis. We applied a nitrogen solution as a spray over the soil, consisting of ammonium bicarbonate, urea, and deionized water, mixed according to local farmland practices. The solution was formulated to simulate local dryland fertilization, with a nitrogen input of 196.1 kg/hm². For a 3 m² experimental area, this amounted to 0.4 kg of ammonium bicarbonate and 0.07 kg of urea. Based on these calculations, the concentration of NH₄⁺-N was determined

to be 344 mg/m². At the preliminary stage of this experiment, a group of soil nitrogen samples were collected every day (Collect 1 kg of soil samples at depths of 10 cm, 20 cm, 40 cm, 60 cm, 80 cm, 100 cm, 120 cm, 140 cm, 155 cm below the surface, a total of 9 samples). With the experiment time expanding, the sampling frequency gradually extended to once a week, and the in situ experiment lasted for 61 days.

The samples were collected in strict accordance with the ‘Technical Specification for Soil Environmental Monitoring’ (HJ/T 166-2004) [41]. The sampling sequence is from bottom to top, with 1 kg of samples collected from each layer, placed in sample bags, and labeled with sample labels and sampling records. There are two copies of the label, one placed in the bag and the other tied to the bag opening. The label indicates the sampling time, location, sample number, monitoring items, and sampling depth. After collection, the samples were sealed, stored at 4 °C, transported back to the laboratory, and frozen at −20 °C. NH₄⁺-N was measured by phenol–hypochlorite spectrophotometry, and nitrate was determined by ultraviolet spectrophotometry. The analyzed method was carried out according to the requirements of the national environmental protection standard of the People’s Republic of China ‘Determination of NH₄⁺-N, NO₃⁻-N and nitrite nitrogen in soil using potassium chloride solution extraction-spectrophotometry’ (HJ 634-2012) [42]. The method for determining the content of NH₄⁺-N and NO₃⁻-N is to first weigh 40.0 g of the soil sample, place it in a 500 mL polyethylene bottle, add 200 mL of potassium chloride solution to the polyethylene bottle, shake and extract for 1 h in a constant temperature water bath oscillator, and maintain the temperature at 20 ± 2 °C. Place 60 mL of the extraction solution into a 100 mL centrifuge tube and centrifuge at 3000 r/min for 10 min. Transfer 50 mL of the supernatant after centrifugation to a 100 mL colorimetric tube to prepare the sample and measure the concentration using a UV spectrophotometer.

2.2. Numerical Model

The HYDRUS-1D model software package (version 4.0) was applied to simulate water flow and solute transport in one-dimensional variable saturated media [43]. In this study, the water flow model was calibrated by soil water content, and the nitrogen migration and transformation were verified by soil nitrogen concentration in the soil profile.

2.2.1. Numerical Description

The water flow governing equation for variably saturated soil water movement is given by the Richards’ equation

$$\frac{\partial \theta}{\partial t} = \frac{\partial}{\partial Z} \left[K(h) \left(\frac{\partial h}{\partial Z} + 1 \right) \right], \quad (1)$$

where θ is the volumetric soil water content (L³ L⁻³); t is the time (T⁻¹); h is the soil water pressure head (L); Z is the vertical space coordinate (L), and K is the hydraulic conductivity function (LT⁻¹). We used van Genuchten’s K - h and θ - h relationships for describing soil hydraulic properties soils:

$$\theta(h) = \theta_r + \frac{\theta_s - \theta_r}{[1 + (\alpha h)^n]^m}, \quad h \leq 0 \quad (2)$$

$$K(h) = K_s S_e^l \left[1 - \left(1 - S_e^{1/m} \right)^m \right]^2, \quad (3)$$

$$m = 1 - \frac{1}{n} \quad \text{and} \quad S_e = \frac{\theta - \theta_r}{\theta_s - \theta_r} \quad (4)$$

where θ_r and θ_s denote the residual and saturated volumetric water contents ($L^3 L^{-3}$), respectively; α (L^{-1}), m (-dimensionless), and n (dimensionless) are fitting parameters of soil–water characteristic curve; l (dimensionless) is the pore connectivity parameter (0.5); K_s (LT^{-1}) is the saturated hydraulic conductivity, and Se (dimensionless) is the relative saturation.

The partial differential equations governing one-dimensional advective–dispersive nitrogen transport and transformations in variably saturated soil are taken as

Urea:

$$\frac{\partial \theta c_{w,1}}{\partial t} = \frac{\partial}{\partial Z} \left(\theta D_1 \frac{\partial c_{w,1}}{\partial Z} \right) - \frac{\partial q c_{w,1}}{\partial Z} - \mu'_{w,1} \theta c_{w,1}, \quad (5)$$

NH_4^+ -N:

$$\begin{aligned} \frac{\partial \theta c_{w,2}}{\partial t} + \rho \frac{\partial c_{s,2}}{\partial t} = & \frac{\partial}{\partial Z} \left(\theta D_2 \frac{\partial c_{w,2}}{\partial Z} \right) - \frac{\partial q c_{w,2}}{\partial Z} + \mu'_{w,1} \theta c_{w,1} - (\mu_{w,2} + \mu'_{w,2}) \theta c_{w,2} \\ & - (\mu_{s,2} + \mu'_{s,2}) \rho c_{s,2} + \gamma_{w,2} \theta + \gamma_{s,2} \rho, \end{aligned} \quad (6)$$

NO_3^- -N:

$$\frac{\partial \theta c_{w,3}}{\partial t} = \frac{\partial}{\partial Z} \left(\theta D_3 \frac{\partial c_{w,3}}{\partial Z} \right) - \frac{\partial q c_{w,3}}{\partial Z} + \mu'_{w,2} \theta c_{w,2} - (\mu_{w,3} + \mu_{s,3}) \theta c_{w,3} + \mu'_{s,2} \rho c_{s,2}, \quad (7)$$

where subscript numbers 5, 6, and 7 denote the nitrogen species (urea, NH_4^+ -N, and NO_3^- -N, respectively), and w and s are the liquid and solid phases of nitrogen. c is the nitrogen concentration (MM^{-1}); ρ is the soil bulk density (ML^{-3}); D is the nitrogen dispersion coefficient ($L^2 T^{-1}$); q is the volumetric water flux (LT^{-1}); μ represents the first-order N transformation rate constant (T^{-1}), while μ' is the similar first-order rate constant providing connections between urea, NH_4^+ -N, and NO_3^- -N; γ is the zero-order nitrogen transformation rate constants ($ML^{-3} T^{-1}$). The dispersion coefficient in the liquid phase D is given by $\theta D = D_L |q| + \theta D_w^0 \tau_w$, where D_w^0 is the molecular diffusion coefficient in free water ($L^2 T^{-1}$), τ_w is the tortuosity factor in the liquid phase, and D_L is the longitudinal dispersivity (L).

The process of NH_4^+ -N adsorption by soil was accounted for utilizing linear adsorption isotherms, which relates c_w and c_s in equation $c_s = K_d \cdot c_w$, where K_d ($L^3 M^{-1}$) is the distribution coefficient of NH_4^+ -N between liquid and solid phase. *Peclet* number (N_{PE}) is a dimensionless number in heat and mass transfer. It is the ratio of convection rate to diffusion rate, which is used to characterize the dominance of convection and diffusion in the vertical migration of pollutants. The dynamics of the nitrogen migration and transformation in the unsaturated zone can be briefly analyzed via *Peclet* number. According to the four types classified by Pfannkuch [44], the *Peclet* number can explain the convection or dispersion dominance (Table 2). The formula to calculate N_{PE} is

$$N_{PE} = \frac{V \times d}{D_w}, \quad (8)$$

where V is Darcy velocity; d is grid spacing; and D_w is the diffusion coefficient.

Table 2. Four types of *Peclet* numbers.

N_{PE}	Solute Migration State
$N_{PE} < 0.01$	Absolute dominance of dispersion
$0.01 < N_{PE} < 4$	Interaction of convective and dispersion
$4 < N_{PE} < 10^4$	Convection dominant
$10^4 < N_{PE} < 10^6$	Absolute convection dominance

2.2.2. Initial and Boundary Conditions

The initial conditions of water flow were determined by the observed soil water content in situ. The initial contents of NH_4^+ -N and NO_3^- -N in soil were also based on the in situ experiment results. The initial concentration of urea was calculated from the initial concentration of the applied fertilizer and initial soil water content, and urea was assumed to be homogeneous in 5 cm soil layer.

The upper boundary condition of the water flow model is selected as the atmospheric boundary with surface runoff, and the lower boundary is chosen as the variable pressure head condition via the groundwater levels measured. Using observation data, the interaction of rainfall, wind speed, irrigation, solar radiation, and fertilization is given under time-varying boundary conditions. The upper boundary condition of the solute transport model is the concentration boundary, and the lower boundary condition is a free flux boundary.

2.2.3. Hydraulic and Solute Transport Parameters

The HYDRUS-1D software package can use soil particle size classification (percentage of sand, silt, and clay) and soil bulk density as input parameters (Table 1). The soil water hydraulic parameters (θ_r , θ_s , α , n , and L) and saturated hydraulic conductivity (K_s) in the van Genuchten model were predicted by a neural network. These parameters need to be calibrated and validated to better simulate soil water movement. The parameter data are listed in Table 3.

Table 3. Statistical measures of HYDRUS-1D model performance for simulation of soil water content, NH_4^+ -N, and NO_3^- -N.

Depth (cm)	RMSE			R ²		
	Soil Water Content	NH_4^+ -N	NO_3^- -N	Soil Water Content	NH_4^+ -N	NO_3^- -N
0–10	0.096			0.711		
10–20	0.007	0.0006	0.0107	0.887	0.9708	0.9543
20–40	0.008	0.0005	0.0080	0.945	0.9715	0.9676
40–60	0.009	0.0007	0.0045	0.863	0.9548	0.9895
60–80	0.007	0.0009	0.0054	0.855	0.9244	0.9981
80–100	0.009	0.0008	0.0038	0.897	0.9407	0.9957
100–120	0.008	0.0005	0.0028	0.911	0.9706	0.9968
120–140	0.005	0.0012	0.0048	0.917	0.9026	0.9895
140–155	0.009	0.0005	0.0053	0.900	0.9424	0.9888
155–410	0.010	0.0005	0.0048	0.856	0.9697	0.9887

2.3. Model Evaluation

The coefficient of determination R^2 and root mean square error (RMSE) were used to evaluate the model simulation results. The RMSE calculation formula is as follows:

$$\text{RMSE} = \sqrt{\frac{\sum_{i=1}^n (s_i - o_i)^2}{n}}, \quad (9)$$

where s_i and o_i are the simulated and observed values of soil water content; NH_4^+ -N and NO_3^- -N are the concentrations of sample i ; n is the total number of the samples. R^2 represents the goodness of fit of the model. The closer the value is to 1, the closer the simulated value is to the actual situation. The RMSE reflects the average absolute error between the simulated value and the observed value. The numerical range is from 0 to positive infinity. The smaller the value, the closer the simulation is to the real conditions.

2.4. Nitrogen Balance Calculation

Based on the principle of nitrogen balance, nitrogen surplus and potential nitrogen losses are determined by calculating the nitrogen input and output from the results of the numerical model [45].

3. Results

3.1. Impact of Rainfall and Groundwater on Nitrogen Migration

3.1.1. Variation in Rainfall and Groundwater Depth

The rainfall and groundwater depth change with time is shown in Figure 3. During this experiment, the maximum rainfall was 11.4 mm/d, and the rainfall on the day of the spray experiment was 6.24 mm. The groundwater table depth changed in response to rainfall at the start of this experiment. It can be seen from Figure 3 that the groundwater depth ranged between 145.5 and 187.9 cm below ground level. On the first day of this experiment, there was no rainfall event, and the groundwater depth was 179.4 cm. The groundwater depth gradually increased from the second day to the sixth day and reached the shallowest value of 145.0 cm below ground level on the sixth day. A rainfall event occurred on the eighth day, but the trend continued downward. Rainfall on days 12 to 16 of this experiment resulted in an increase in groundwater level. From the 17th to the 48th day, only a few days of light rain occurred, and groundwater depth declined continuously with slight fluctuation. Despite rainfall events occurring between days 48 and 54, groundwater levels continued to decline, reaching the deepest value of 187.9 cm below ground level on the 61st day.

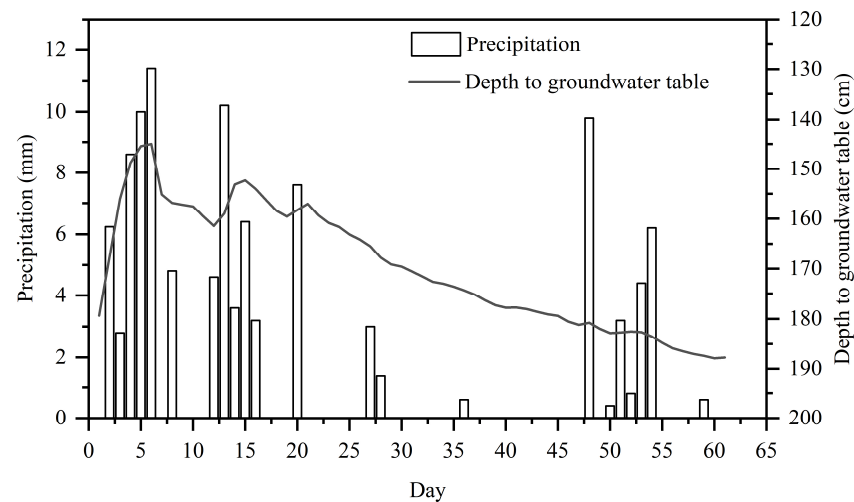


Figure 3. Changes in daily rainfall and depth to groundwater table during the experiment period.

3.1.2. The Effect of Precipitation on the Nitrogen Migration

From Table 2, it can be seen that the Peclet number is greater than 0.01, and the convection and dispersion work together. If it is less than 0.01, then the dispersion is dominant. When it is greater than 4, the convection is dominant. Based on this, the dominance of convective and dispersion of nitrogen process affected by precipitation was analyzed. It can be seen from Figure 4 that the N_{PE} value fluctuates in the range of 0.05–12 during the experiment period. The Peclet number of this experiment was 0.24 on the first day. The Peclet number reached a maximum value of 11.58 during the application of nitrogen solution, indicating that convection dominated. Most of the time in the experiment period, the Peclet number fluctuated between 0.01 and 4, which means that the migration of nitrogen was controlled by both convection and dispersion. It was found that the Peclet number changed with rainfall. The Peclet number value increased during rainfall and decreased during periods with no precipitation.

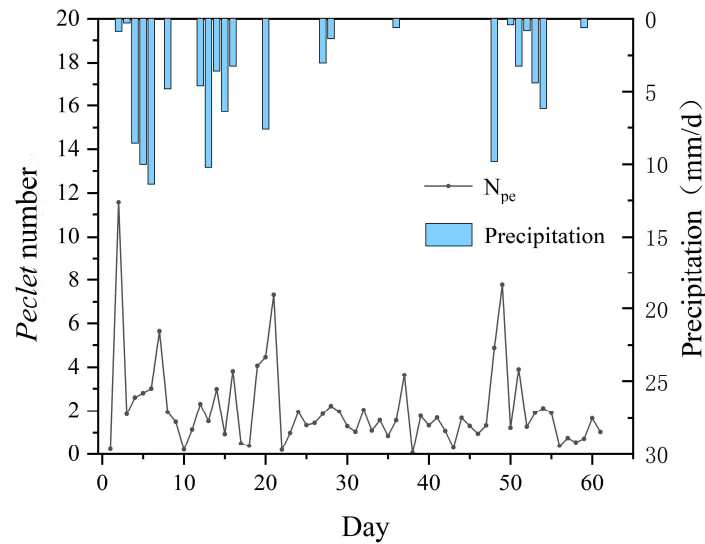


Figure 4. Pecler number changes with precipitation during the experiment period.

3.2. Model Verification of Soil Water Content and Nitrogen

The fit of simulated and observed soil water contents of each layer are shown in Figure 5. It can be seen that the soil water contents are well-fitted except for the surface layer. The surface layer is easily disturbed by the external environment in the air–soil interface, so the divergence between the observed data and the simulated data is expected. The RMSE of the model was acceptable for all, but the surface layer, and the R^2 was greater than 0.85, indicating that the simulated values were in good agreement with the measured values, which could be applied to the simulation of soil water movement in the experiment site.

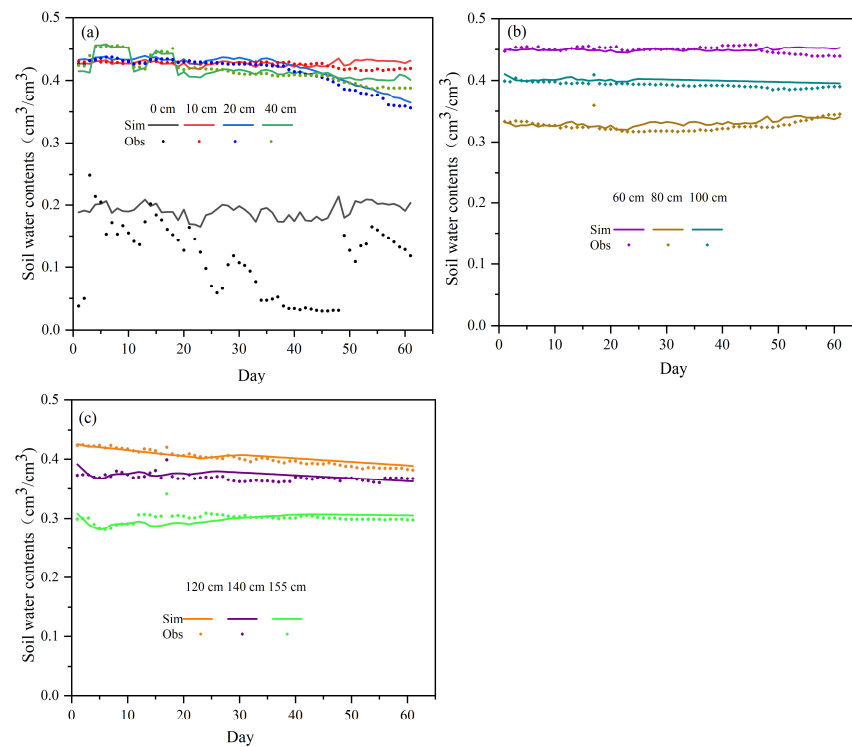


Figure 5. The fit of observed and simulated soil water contents at different soil depths. (a) presents the fit of observed and simulated soil water contents at soil depths of 0 cm, 10 cm, 20 cm, and 40 cm; (b) shows the fit of observed and simulated soil water contents at soil depths of 60 cm, 80 cm, and 100 cm; (c) displays the fit of observed and simulated soil water contents at soil depths of 120 cm, 140 cm, and 155 cm. Sim—simulated; Obs—observed.

The output of NO_3^- -N concentration in this model is the liquid phase concentration, and the liquid phase concentration and the total soil NO_3^- -N concentration measured in the field are converted using the following formula:

$$C_w = \frac{C_s \gamma}{1000\theta} \quad (10)$$

where C_w is the NO_3^- -N concentration in soil solution (mg/cm^3); C_s is the NO_3^- -N concentration in air-dried soil sample (mg/kg); γ is soil bulk density (g/cm^3); θ is the soil volumetric water content (cm^3/cm^3).

The fit of observed and simulated NH_4^+ -N and NO_3^- -N are shown in Figures 6 and 7, respectively. Overall, the fitting is good except for a deviation between the simulated and the measured NH_4^+ -N at a depth of 60 cm. The RMSE of the remaining layers was less than 0.01, and the R^2 was greater than 0.85 (Table 3).

This indicates that the simulated value is in good agreement with the measured value, which could be applied to the simulation of nitrogen migration and transformation in the research soil profile.

This model involves multiple parameters of soil solute transport and transformation. On the basis of the parameter sensitivity test and previous studies on solute migration and transformation, the values of the model's soil solute transport and transformation parameters are shown in Table 4.

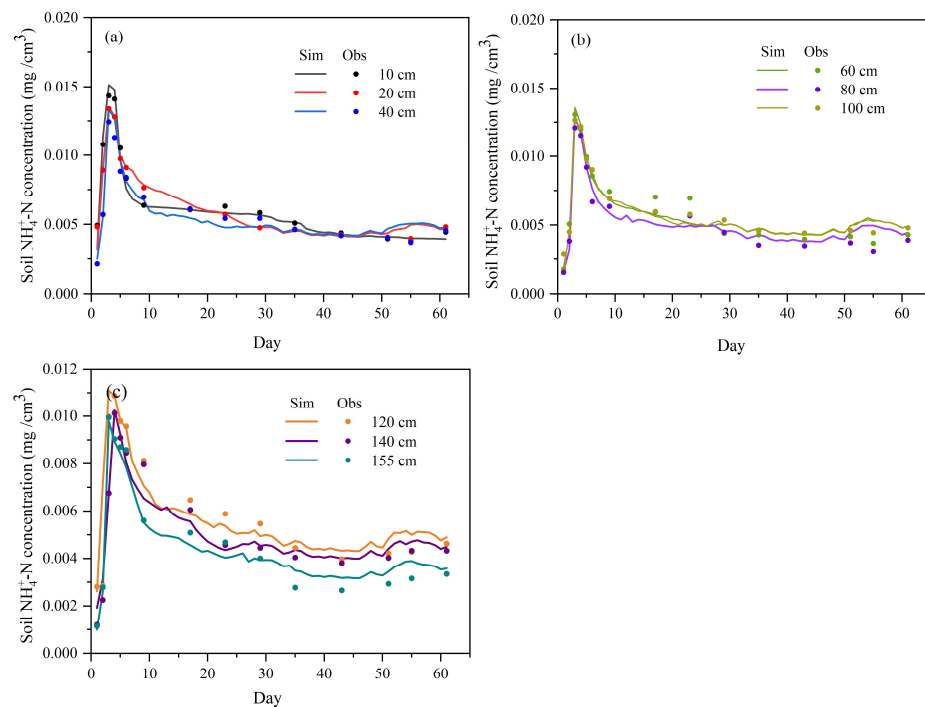


Figure 6. Variations in soil NH_4^+ -N at different soil depths. (a) presents the variations in soil NH_4^+ -N at soil depths of 0 cm, 10 cm, 20 cm, and 40 cm; (b) shows the variations in soil NH_4^+ -N at soil depths of 60 cm, 80 cm, and 100 cm; (c) displays the variations in soil NH_4^+ -N at soil depths of 120 cm, 140 cm, and 155 cm. Sim—simulated; Obs—observed.

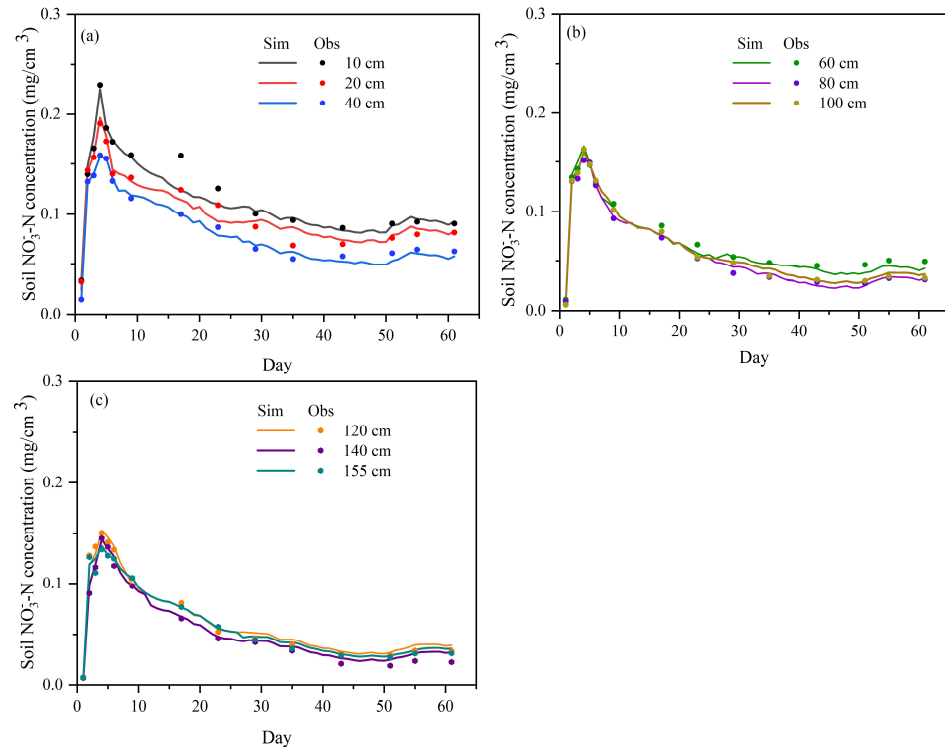


Figure 7. Variations in soil NO₃⁻-N at different soil depths. (a) presents the variations in soil NO₃⁻-N at soil depths of 0 cm, 10 cm, 20 cm, and 40 cm; (b) shows the variation in soil NO₃⁻-N at soil depths of 60 cm, 80 cm, and 100 cm; (c) displays the variation in soil NO₃⁻-N at soil depths of 120 cm, 140 cm, and 155 cm. Sim—simulated; Obs—observed.

Table 4. Calibrated parameters of the numerical model at different depths.

Depth (cm)	θ_r (cm ³ ·cm ⁻³)	θ_s (cm ³ ·cm ⁻³)	α (cm ⁻¹)	n [-]	K_s (cm·min ⁻¹)	L [-]	D_L (cm)	K_d	$\mu'_{w,1}$ (d ⁻¹)	$\mu_{w,2}$ (d ⁻¹)	$\mu'_{w,2}$ (d ⁻¹)	$\mu'_{s,2}$ (d ⁻¹)	$\mu_{w,3}$ (d ⁻¹)	$\mu_{s,3}$ (d ⁻¹)
0–10	0.03	0.30	0.0079	1.531	10.0	0.5	7	0.50	0.35	0.04	0.070	0.070	0.001	0.001
10–20	0.03	0.46	0.0050	1.100	10.3	0.5	14	0.50	0.32	0.02	0.062	0.062	0.001	0.001
20–40	0.03	0.47	0.0060	1.100	11.8	0.5	10	0.50	0.18	0.02	0.060	0.060	0.001	0.001
40–60	0.03	0.50	0.0050	1.200	10.8	0.5	12	0.50	0.17	0.02	0.060	0.060	0.002	0.002
60–80	0.03	0.50	0.0050	1.100	12.0	0.5	12	0.50	0.17	0.01	0.042	0.042	0.002	0.002
80–100	0.03	0.45	0.0110	1.300	11.5	0.5	10	0.15	0.17	0.01	0.038	0.038	0.002	0.002
100–120	0.03	0.50	0.0100	1.300	10.0	0.5	10	0.10	0.17	0.01	0.038	0.038	0.002	0.002
120–140	0.03	0.47	0.0080	1.300	10.0	0.5	10	0.10	0.17	0.01	0.038	0.038	0.002	0.002
140–155	0.03	0.45	0.0070	1.600	10.0	0.5	11	0.10	0.17	0.01	0.038	0.038	0.002	0.002
155–410	0.03	0.33	0.0060	2.600	10.0	0.5	8	0.10	0.17	0.01	0.038	0.038	0.002	0.002

3.3. Temporal and Spatial Variation in Soil Water Content

The variation in water content with time and depth is shown in Figure 8. Two zones with high soil water content occurred at the depths of 40–60 cm and 100 cm, 0.46 cm³/cm³ and 0.4 cm³/cm³, respectively. Soil water contents were low at the depths of 0 to 10 cm near the ground surface, with a minimum of 0.17 cm³/cm³, and from 10 to 60 cm depth water content gradually increased and ranged around 0.4 cm³/cm³ to 0.45 cm³/cm³, with a maximum value of 0.46 cm³/cm³ and a minimum value of 0.36 cm³/cm³. Soil water content decreased to 0.3 cm³/cm³ at 80 cm, rebounding to about 0.4 cm³/cm³ at 100 cm while decreasing to 0.298 cm³/cm³ at 155 cm. During the experimental period, on the whole, soil water content was high, and the unsaturated zone remained in a quasi-saturated state. When rainfall events occurred, the unsaturated zone acted as a channel, so rainfall had little effect on soil water content but a greater impact on groundwater depth.

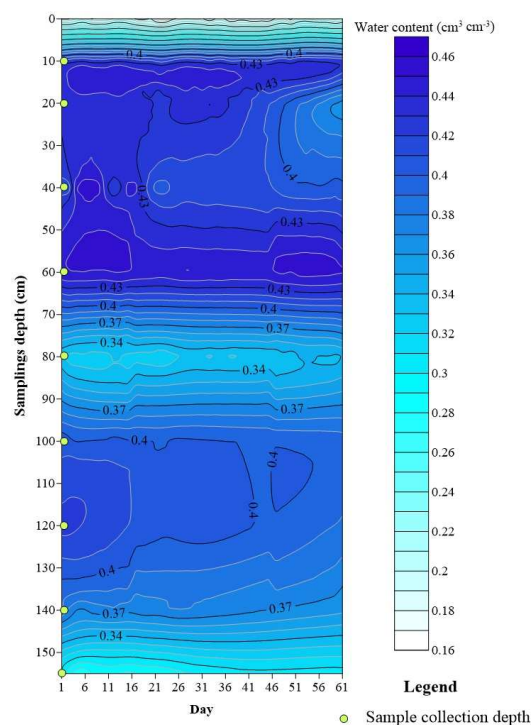


Figure 8. Temporal and spatial variation in soil water contents.

3.4. Distribution of Nitrogen

The variation in NH_4^+ -N concentration with time and depth is shown in Figure 6. NH_4^+ -N concentration increased first and then decreased with time, overall gradually decreasing with depth. The highest content at 10 cm occurred on the third day with 0.02 mg/cm^3 . The concentration at 80 cm was lower than that at 100 cm, and it dropped to the lowest at 155 cm. On the first day of this experiment, the background concentration of NH_4^+ -N in the soil was low. After the application of a solution of ammonium bicarbonate and urea, the concentration increased rapidly at 10 cm and reached the maximum value of 0.02 mg/cm^3 on the 3rd day, then decreased gradually with time but did not return to the background value by the 61st day. In this experiment, the solution applied is a mix of ammonium bicarbonate (inorganic fertilizer) and urea (organic fertilizer). Over time, urea migrated downward and transformed into NH_4^+ -N due to mineralization. The concentration of NH_4^+ -N was still very high on the third day at 20 cm. While precipitation recharge occurred during the experimental period, the soil water content changed only slightly. As a result, NH_4^+ -N did not decrease rapidly to the background value in the shallow layer.

As shown in Figure 7, NO_3^- -N in the profile overall shows a gradual decreasing trend. In the first experiment, the background value concentration of NO_3^- -N in the soil was low. After the application of the test solution, it reached the maximum value of 0.23 mg/cm^3 on the fourth day and then gradually decreased with time. NO_3^- -N concentration was still high on the 61st day and did not return to the background value. As can be seen from Figure 7, NO_3^- -N migrated downward with water from the 1st to the 20th day of this experiment, resulting in an increase in leaching loss. The content of NO_3^- -N in the unsaturated zone gradually decreased to 0.05 mg/cm^3 by 23 days. There were only a few days of rainfall from the 23rd day to the 61st day. The subsequent migration rate of NO_3^- -N was very slow, resulting in a small difference between the concentration of NO_3^- -N on the 61st day and the 22nd day, indicating that NO_3^- -N was prone to leaching with water.

3.5. Mass Balance of Water and Nitrogen

3.5.1. Water Balance

The total amount of water input in the numerical model is 160 mm; water loss accounts for 60.1% of the total water input in the lower boundary, and the water evaporation is 35.5% of the total water input, based on the actual measurement results from the in situ experiments at the site. It can be seen that water loss is mainly the downward movement of soil water compared to evaporation. That indicates that precipitation mainly recharges to groundwater, and nitrogen migrates easily to groundwater. The total water balance error of the model is 0.462 cm, and the relative error is 2.9%, which means that the numerical results of the model are reliable.

3.5.2. Nitrogen Balance

The results of the model simulation of soil ammonia nitrogen mass conservation during this experiment are shown in Figure 9. The input NH_4^+ -N includes ammonium bicarbonate and urea (Figure 9a). The output is NO_3^- -N, NH_4^+ -N migration with water and soil residual NH_4^+ -N. The upper part of the figure is the output component, and the lower part is the input component. The nitrogen balance pie charts for days 1, 10, 30, and 61 are shown below. It can be seen from the chart that the background value on the first day was 22.1% and gradually decreased to 1.5%. Ammonium bicarbonate hydrolysis reached a maximum value of 83.8% on day 10 and then gradually decreased to 43.9% on day 61. Urea hydrolysis accounted for 75.5% on day 1, then gradually decreased to 15.5%, and then increased to 54.6% on day 61. This confirms that the input NH_4^+ -N is mainly ammonium bicarbonate and urea, in which ammonium carbonate gradually decreases with time, and urea remains in the soil at a higher concentration. The output components were soil residue, leakage, and nitrification. At the initial period of application, the soil residue accounted for 88.7%. Over time and with nitrification, it gradually decreased to 6.1% by the 61st day. Moreover, the leakage amount was only 3% on the first day and less than 0.3% on the remaining days of this experiment. Nitrification occurs after NH_4^+ -N enters the soil, and the process increases over time, thus accounting for the increase from 8.3% to 85.3% on days 1 and 61, respectively.

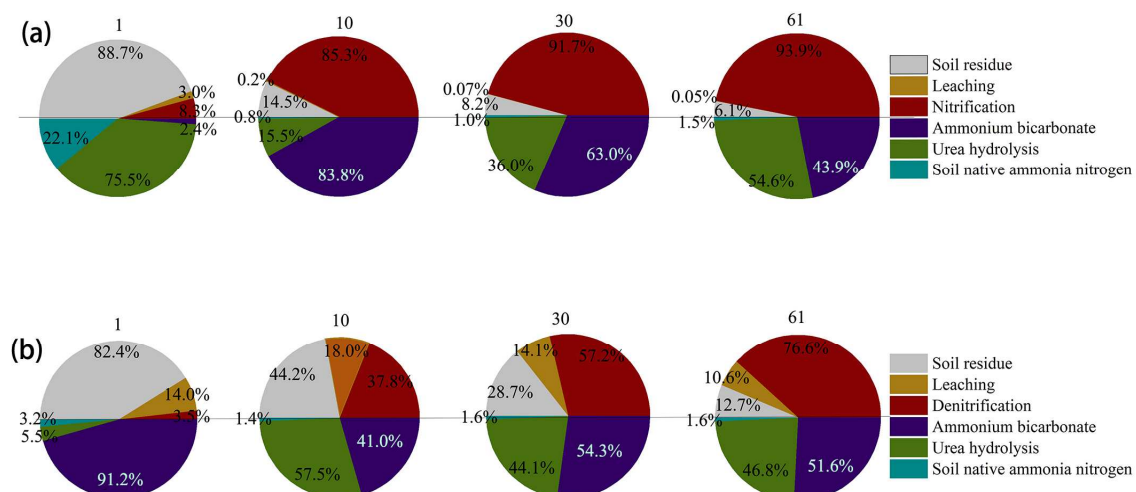


Figure 9. Nitrogen balance during the experiment period. (a) represents the NH_4^+ -N balance; (b) represents the NO_3^- -N balance.

NO_3^- -N balance analysis is shown in Figure 9b. The inputs include NH_4^+ -N, urea hydrolysis (conversion through NO_3^- -N nitrification), and soil background values. The outputs include nitrate denitrification to N_2 , nitrate leaching with water, and soil residue.

Similar to the NH_4^+ -N balance pie chart, the upper part is the output, and the lower part is the input component. It can be seen that the background value on the first day was 3.2%, then decreased to 1.4% on the tenth day, and subsequently remained at 1.6%. The ratio of ammonium bicarbonate hydrolyzed to NH_4^+ -N and then converted to nitrate reached the maximum value of 91.2% on the 1st day and then decreased to 51.6% on the 61st day. The ratio of urea hydrolyzed to NH_4^+ -N and then converted to nitrate was 5.5% on the first day, gradually increased to 57.5% on the 10th day, and decreased to 46.8% on the 61st day. In the initial period of the nitrogen fertilizer application, the soil residue accounted for 82.4%. With the reaction of nitrification and leakage over time, it gradually decreased to 12.7% by the 61st day. The losses account for 14% to 18%, which indicates that nitrate is less easily adsorbed by soil than NH_4^+ -N. The denitrification reaction became dominant over time as this process increased from 3.5% to 76.6% over the 61 days monitored.

4. Discussion

4.1. Analysis of Distribution Characteristics of NH_4^+ -N and NO_3^- -N Pollutants

According to previous studies [7,46], clay has strong adsorption of ammonia nitrogen, and in general, NH_4^+ -N accumulates in large quantities in the shallow layer of soil and decreases rapidly with the buried depth. However, due to the addition of ammonium bicarbonate (inorganic fertilizer) and urea (organic fertilizer) at the same time in this experiment, ammonium bicarbonate is directly converted into NH_4^+ -N when it meets water, while urea requires mineralization to transform. Therefore, ammonium bicarbonate was applied on the second day of this experiment, and soil NH_4^+ -N concentration was higher at 10 cm. Urea migrated downward with time and was converted into NH_4^+ -N due to mineralization, and NH_4^+ -N concentration reached the maximum at 20 cm on the third day. As can be seen from Figure 3, during this experiment, there was more rainfall, but the water content changed little with time, and the groundwater depth changed significantly. According to Figure 8, except for the surface layer, the moisture content of the other layers is relatively high and reaches a near-saturation state, and the moisture resistance of each layer in the clay-unsaturated zone decreases during rainfall. As can be seen from Figure 6, NH_4^+ -N does not decrease to the background value immediately after accumulation in the shallow layer, and part of NH_4^+ -N is adsorbed in the shallow layer. In contrast, the other part migrates to the lower layer with water. The NH_4^+ -N concentration at 80 cm is lower than that at 100 cm because the soil moisture content at 80 cm is low, about $0.30 \text{ cm}^3/\text{cm}^3$. The higher oxygen content in the soil at 80 cm probably promotes nitrification, converting NH_4^+ -N into nitrate nitrogen. Meanwhile, water movement accelerates NH_4^+ -N accumulation at 100 cm. As depth increases, soil density rises, and oxygen content decreases. Nitrification slows down while denitrification intensifies. This likely results in slower NH_4^+ -N decay rates in deeper layers compared to shallow ones. Consequently, NH_4^+ -N concentrations gradually decrease below 100 cm. However, the concentration at 155 cm is higher than at 140 cm, possibly because 155 cm lies within the water fluctuation zone, where conditions promote both nitrification and denitrification, leading to higher NO_3^- -N levels.

As can be seen from Figure 7, soil NO_3^- -N concentration is not easily adsorbed by soil and is easily lost with water. The change in soil NO_3^- -N concentration is more pronounced than that of soil NH_4^+ -N concentration, but significant differences are primarily observed in the shallow soil layer, indicating that the adsorption capacity of NO_3^- -N in soil is weak, so it is easy to be lost with water. Soil NO_3^- -N concentration showed a gradually decreasing trend. Before the start of this experiment (first day), the background value concentration of NO_3^- -N in the soil was low. After applying ammonium bicarbonate and urea, the NO_3^- -N content at 10 cm increased rapidly, reaching a peak of $0.2255 \text{ mg}/\text{cm}^3$ on the

fourth day. This was because the 10 cm layer was close to the surface, allowing for efficient oxygen exchange with the atmosphere, which accelerated nitrification and converted a large amount of $\text{NH}_4^+\text{-N}$ into $\text{NO}_3^-\text{-N}$. The nitrification reaction rate is fast, and a large amount of $\text{NH}_4^+\text{-N}$ can be converted into $\text{NO}_3^-\text{-N}$; the $\text{NO}_3^-\text{-N}$ content reaches its highest level at the 10 cm depth. In Figure 3, the concentration of $\text{NO}_3^-\text{-N}$ in the clay-unsaturated zone decreased rapidly during heavy rainfall and more slowly during light rainfall. This suggests that rainfall contributes to $\text{NO}_3^-\text{-N}$ leaching along with soil moisture. However, in clay-rich soil with low permeability, rainfall may also enhance denitrification, which could further reduce $\text{NO}_3^-\text{-N}$ levels. As soil depth increases, oxygen content decreases, nitrification slows, and denitrification intensifies, leading to a gradual decline in $\text{NO}_3^-\text{-N}$ concentration below 80 cm.

4.2. The Influence of Shallow Groundwater Table on Nitrogen Migration

In this study, migration and transformation of nitrogen in clay-rich soil under shallow groundwater depth were studied by in situ test; furthermore, numerical simulation was conducted to verify the experimental data. The RMSE of measured and simulated soil moisture content, except for the surface layer, is less than 0.01, while the RMSE for $\text{NH}_4^+\text{-N}$ and $\text{NO}_3^-\text{-N}$ is less than 0.011. The R^2 values for soil moisture content, excluding the surface layer, are above 0.85, and for $\text{NH}_4^+\text{-N}$ and $\text{NO}_3^-\text{-N}$, they are above 0.9, indicating good model fitting. As shown in Figure 5, the soil moisture content fits well for layers other than the surface layer. This discrepancy at the surface may be attributed to its susceptibility to external environmental disturbances, leading to differences between measured and simulated data. Figures 6 and 7 show that the trends for $\text{NH}_4^+\text{-N}$ and $\text{NO}_3^-\text{-N}$ exhibit an initial increase followed by a decrease. The discrepancy between measured and simulated $\text{NH}_4^+\text{-N}$ data at 60 cm may result from the model's inability to accurately simulate the processes of mineralization and nitrification. It was found that, except for the surface layer, the moisture content of each layer of the soil changed little with time (Figure 8). The lower water content is due to evaporation and infiltration. Because the lower soil has higher density and smaller pores, the water content gradually decreases. The shallow layer is also affected by evaporation and infiltration, and the water content is also lower, resulting in the highest water content at a depth of 60 cm. On the whole, the water content is high, the clay-unsaturated zone is close to saturation state, and the rainfall mainly promotes leaching. According to the measured data, the groundwater depth is between 145.5 and 187.9 cm, and the groundwater depth at the experiment site is controlled by precipitation (Figure 3). The groundwater depth decreases during rainfall and increases when there is no rainfall. Specifically, a shallower groundwater table will facilitate the easier entry of $\text{NH}_4^+\text{-N}$ into the groundwater system, and $\text{NH}_4^+\text{-N}$ also becomes a potential source of groundwater pollution in a humid environment [47,48]. Because of its low permeability, clay is often used as a barrier to prevent pollutants from seeping into groundwater, but its effectiveness needs to be proven in shallow groundwater conditions. The in situ experiment was located in the Hanjiang River basin under humid climate conditions, with an average annual precipitation of 855.3 mm, an average relative humidity of 79%, and a relatively high soil water content ranging between 0.30 and 0.45 cm^3/cm^3 . In dry clay soils, fractures and cracks can serve as preferential conduits for the rapid transport of water and solutes into the unsaturated zone, especially during heavy rains or flood events when local runoff accumulates and seeks paths of least resistance [49,50]. During rainfall, due to the quasi-saturation of soil water content, the unsaturated zone only acts as the corridor of water movement. Water is easy to migrate downward, and nitrogen ($\text{NH}_4^+\text{-N}$, $\text{NO}_3^-\text{-N}$) is also easy to migrate downward with water, polluting groundwater.

In Figure 4, when the N_{PE} value increases to more than 4 during rainfall, convection gradually dominates. That is, during rainfall, nitrogen is transported downward faster with soil water, and thus, nitrogen migration is greatly affected by rainfall. In contrast, when the N_{PE} value varied between 0.01 and 4 during periods of no precipitation, convection and dispersion performed together, and the downward migration of nitrogen slowed down.

4.3. Control of the Effect of Clay-Unsaturated Zone on the Migration and Transformation of Nitrogen Pollutants

The strong adsorption of $\text{NH}_4^+\text{-N}$ by clay depends on the mineral composition of the clay [51]. Clay is mainly formed by silicate minerals after weathering on the earth's surface, and its mineral composition includes the kaolinite group, montmorillonite group, illite group, and chlorite group. On the one hand, clay minerals can adsorb $\text{NH}_4^+\text{-N}$ through ion exchange, resulting in strong adsorption by clay. In the expandable lattice of 2:1 clay minerals such as montmorillonite, the unit interlayer cations (Ca^{2+} , Mg^{2+} , Na^+ , K^+) can be replaced by NH_4^+ , giving rise to ammonium fixation clays [52,53]. On the other hand, the surface of clay minerals has rich functional groups (such as hydroxyl, silico-oxygen bond, etc.), which can chemically react with $\text{NH}_4^+\text{-N}$ to form chemical bonding to achieve adsorption. In addition, the negative charge on the surface of clay minerals can also attract positively charged NH_4^+ ions, which can be adsorbed by electrostatic action. Different types of clay minerals have different adsorption capacities for $\text{NH}_4^+\text{-N}$ [54–56]. For example, montmorillonite clay minerals have a large specific surface area and a strong ion exchange capacity, so they have a strong adsorption capacity for $\text{NH}_4^+\text{-N}$. The smaller the clay mineral particles, the larger the specific surface area and the stronger the adsorption capacity of $\text{NH}_4^+\text{-N}$. Therefore, clay, as a weak permeable layer, is generally believed to have a blocking effect on the entry of pollutants into groundwater. However, previous studies have not considered the migration and transformation of nitrogen in the near-saturated state and ignored the control of the structure of the clay-unsaturated zone on the migration and transformation of pollutants [57,58]. The presented results show that the retarding effect of the clay-unsaturated zone on nitrogen pollutants varies under the influence of groundwater depth, unsaturated zone thickness, and unsaturated zone water content. When the water content of the clay-unsaturated zone is high (near saturation), its permeability increases, and its barrier effect decreases. In this case, the clay-unsaturated zone primarily serves as a pathway for water migration, and $\text{NH}_4^+\text{-N}$ and $\text{NH}_4^+\text{-N}$ are more likely to move downward into the groundwater along with water during rainfall.

This study verified nitrogen migration and transformation in clay-rich soil under shallow water tables through tests and simulations, but deeper insights into chemical reactions, ion exchange, and adsorption differences among clay minerals influenced by environmental factors are needed. Comprehensive assessments are required to identify optimal clay types and barrier structures for effective groundwater pollution control. This study enhanced understanding of nitrogen fertilizer conversion in shallow groundwater, offered optimization suggestions, promoted nitrogen fertilizer research, and supported sustainable agriculture.

5. Conclusions

This study investigated nitrogen migration and transformation in clay-rich soil with a shallow groundwater table in a humid climate area by combining an in situ experiment with numerical simulation. Generally, although $\text{NH}_4^+\text{-N}$ was adsorbed by clay in large quantities in the silt–clay soil, a significant 10–15% was still lost to groundwater despite the presence of clay-rich soils. This differs from the traditional knowledge of nitrogen migration and transformation features, which assumes clay-rich soils to be an impenetrable

barrier for the prevention and mitigation of pollution to groundwater. However, in the case of silt clay soils, these soils were not as impermeable as assumed in many studies.

- (1) Peak concentrations of NH_4^+ -N occurred earlier (on the third day) than NO_3^- -N (on the fourth day);
- (2) By the end of this experiment, the concentrations of both ammonia and NO_3^- -N had not returned to background concentrations;
- (3) The depth of the groundwater table fluctuated between 145.5 and 187.9 cm below ground level. Consequently, NH_4^+ -N and NO_3^- -N were able to migrate downward and then enter the groundwater convected by precipitation recharge;
- (4) The pattern of nitrogen migration is dominated by convection during precipitation, while convection and dispersion act together during dry periods, according to the Peclet number;
- (5) The leakage loss of NO_3^- -N in soil accounts for 14% to 18%. The nitrification reaction of NH_4^+ -N and NO_3^- -N is rapid over time, with increases from 8.3% to 85.3% and from 3.5% to 76.6%, respectively.

To sum up, more attention should be paid to the prevention of nitrogen pollution in humid climate areas with shallow groundwater tables even though the unsaturated zone is clay-rich soil, as this may not provide the protection originally thought.

Author Contributions: Conceptualization, J.H. and Q.L.; methodology, J.H. and Q.L.; software, Z.Y.; validation, F.P., J.W. and G.S.; formal analysis, T.H.; investigation, Z.L.; resources, T.F.; data curation, F.Z.; writing—original draft preparation, F.P.; writing—review and editing, Q.L.; visualization, Q.L.; supervision, F.S.; project administration, J.H.; funding acquisition, J.H. All authors have read and agreed to the published version of the manuscript.

Funding: This research was supported by the National Natural Science Foundation of China (42177076, 41672250) and the Natural Science Foundation of Shaanxi Province (2021ZDLSF05-09).

Data Availability Statement: Data are available upon request from the authors.

Acknowledgments: The authors thank three anonymous reviewers for their detailed and helpful comments on improving this paper.

Conflicts of Interest: The authors declare that they have no known competing financial interests or personal relationships that could have appeared to influence the work reported in this paper.

References

1. Castaldelli, G.; Colombani, N.; Tamburini, E.; Vincenzi, F.; Mastrocicco, M. Soil type and microclimatic conditions as drivers of urea transformation kinetics in maize plots. *Catena* **2018**, *166*, 200–208. [[CrossRef](#)]
2. Li, Y.; Šimůnek, J.; Zhang, Z.; Jing, L.; Ni, L. Evaluation of nitrogen balance in a direct-seeded-rice field experiment using Hydrus-1D. *Agric. Water Manag.* **2015**, *148*, 213–222. [[CrossRef](#)]
3. Weitzman, J.N.; Brooks, J.R.; Compton, J.E.; Faulkner, B.R.; Mayer, P.M.; Peachey, R.E.; Rugh, W.D.; Coulombe, R.A.; Hatteberg, B.; Hutchins, S.R. Deep soil nitrogen storage slows nitrate leaching through the vadose zone. *Agric. Ecosyst. Environ.* **2022**, *332*, 107949. [[CrossRef](#)]
4. Ascott, M.J.; Gooddy, D.C.; Wang, L.; Stuart, M.E.; Lewis, M.A.; Ward, R.S.; Binley, A.M. Global patterns of nitrate storage in the vadose zone. *Nat. Commun.* **2017**, *8*, 1416. [[CrossRef](#)]
5. Xin, J.; Liu, Y.; Chen, F.; Duan, Y.; Wei, G.; Zheng, X.; Li, M. The missing nitrogen pieces: A critical review on the distribution, transformation, and budget of nitrogen in the vadose zone-groundwater system. *Water Res.* **2019**, *165*, 114977. [[CrossRef](#)]
6. Liang, X.; Tian, G.; Li, H.; Chen, X.; Zhu, S. Characteristics of nitrogen and phosphorus runoff loss in paddy field under natural rainfall conditions. *J. Soil Water Conserv.* **2005**, *1*, 59–63, (In Chinese with English abstract).
7. Mo, X.; Peng, H.; Xin, J.; Wang, S. Analysis of urea nitrogen leaching under high-intensity rainfall using HYDRUS-1D. *J. Environ. Manag.* **2022**, *312*, 114900. [[CrossRef](#)]
8. Xiao, M.; Li, Y.; Wang, J.; Hu, X.; Wang, L.; Miao, Z. Study on the law of nitrogen transfer and conversion and use of fertilizer nitrogen in paddy fields under water-saving irrigation mode. *Water* **2019**, *11*, 218. [[CrossRef](#)]

9. Yang, R.; Tong, J.; Hu, B.X.; Li, J.; Wei, W. Simulating water and nitrogen loss from an irrigated paddy field under continuously flooded condition with Hydrus-1D model. *Environ. Sci. Pollut. Res.* **2017**, *24*, 15089–15106. [[CrossRef](#)]
10. Zhou, J.B.; Xi, J.G.; Chen, Z.J.; Li, S.X. Leaching and transformation of nitrogen fertilizers in soil after application of N with Irrigation: A Soil Column Method. *Pedosphere* **2006**, *16*, 245–252. [[CrossRef](#)]
11. Bollmann, A.; Conrad, R. Influence of O₂ availability on NO and N₂O release by nitrification and denitrification in soils. *Glob. Change Biol.* **1998**, *4*, 387–396. [[CrossRef](#)]
12. Mekala, C.; Nambi, I.M. Understanding the hydrologic control of N cycle: Effect of water filled pore space on heterotrophic nitrification, denitrification and dissimilatory nitrate reduction to ammonium mechanisms in unsaturated soils. *J. Contam. Hydrol.* **2017**, *202*, 11–22. [[CrossRef](#)]
13. Wang, X.H.; Liu, Y. Experimental study on purification of reclaimed water by river sediment under different pH conditions. *J. Ecol. Rural Environ.* **2022**, *38*, 1181–1187.
14. Yu, S.; Ehrenfeld, J.G. The effects of changes in soil moisture on nitrogen cycling in acid wetland types of the New Jersey Pinelands (USA). *Soil Biol. Biochem.* **2009**, *41*, 2394–2405. [[CrossRef](#)]
15. Brar, H.S.; Bhullar, M.S. Nutrient uptake by direct seeded rice and associated weeds as influenced by sowing date, variety and weed control. *Indian J. Agric. Res.* **2013**, *47*, 353–358.
16. Gu, Y.; Sun, D.B.; Wang, Q.S. Studies on groundwater nitrate nitrogen distribution and it's affecting factors in Chao lake watershed. *J. Agric. Sci. Technol.* **2011**, *13*, 68–74.
17. Jiao, P.J.; Wang, S.L.; Xu, D.; Wang, Y.Z. Effect of crop vegetation type on nitrogen and phosphorus runoff losses from farmland in one rainstorm event. *Shuili Xuebao/J. Hydraul. Eng.* **2009**, *40*, 296–302.
18. Peng, S.; He, Y.; Yang, S.; Xu, J. Effect of controlled irrigation and drainage on nitrogen leaching losses from paddy fields. *Paddy Water Environ.* **2015**, *13*, 303–312. [[CrossRef](#)]
19. Tafteh, A.; Sepaskhah, A.R. Application of HYDRUS-1D model for simulating water and nitrate leaching from continuous and alternate furrow irrigated rapeseed and maize fields. *Agric. Water Manag.* **2012**, *113*, 19–29. [[CrossRef](#)]
20. Tan, X.; Shao, D.; Gu, W.; Liu, H. Field analysis of water and nitrogen fate in lowland paddy fields under different water managements using HYDRUS-1D. *Agric. Water Manag.* **2015**, *150*, 67–80. [[CrossRef](#)]
21. Alhaj Hamoud, Y.; Guo, X.; Wang, Z.; Shaghaleh, H.; Chen, S.; Hassan, A.; Bakour, A. Effects of irrigation regime and soil clay content and their interaction on the biological yield, nitrogen uptake and nitrogen-use efficiency of rice grown in southern China. *Agric. Water Manag.* **2019**, *213*, 934–946. [[CrossRef](#)]
22. Jarvis, N.; Etana, A.; Stagnitti, F. Water repellency, near-saturated infiltration and preferential solute transport in a macroporous clay soil. *Geoderma* **2008**, *143*, 223–230. [[CrossRef](#)]
23. Karup, D.; Moldrup, P.; Paradelo, M.; Katuwal, S.; Norgaard, T.; Greve, M.H.; de Jonge, L.W. Water and solute transport in agricultural soils predicted by volumetric clay and silt contents. *J. Contam. Hydrol.* **2016**, *192*, 194–202. [[CrossRef](#)]
24. Tian, L.Y.; Wang, S.Q.; Wei, S.C.; Liu, B.X.; Liu, B.B.; Hu, C.S. Effect of the thickness of clay layer in the layered vadose zone on nitrate nitrogen migration. *Trans. Chin. Soc. Agric. Eng.* **2020**, *36*, 55–62.
25. Dong, P.; Li, Y.; Sun, Y.; Xie, Z.H.; Liu, Y.C. Experimental study on the filtration capability of clayey soils in the vadose zone prevention nitrogen from polluting groundwater. *Geoscience* **2016**, *30*, 688–694.
26. Liu, X.; Zuo, R.; Meng, L.; Li, P.; Li, Z.P.; He, Z.K.; Li, Q.; Wang, J.S. Study on the variation law of nitrate pollution during the rise of groundwater level. *China Environ. Sci.* **2021**, *41*, 232–238.
27. Pu, F.; Huang, J.T.; Song, G.; Wang, J.W.; Li, Z.Z.; Tian, H.; Zhang, F.; Sun, F.Q. Movement and transformation of nitrogen in clay unsaturated zone under shallow groundwater table: In-situ experiment. *China Environ. Sci.* **2022**, *42*, 2707–2713.
28. Antonopoulos, V.Z. Modelling of water and nitrogen balances in the ponded water and soil profile of rice fields in Northern Greece. *Agric. Water Manag.* **2010**, *98*, 321–330. [[CrossRef](#)]
29. Chowdary, V.M.; Rao, N.H.; Sarma, P.B.S. A coupled soil water and nitrogen balance model for flooded rice fields in India. *Agric. Ecosyst. Environ.* **2004**, *103*, 425–441. [[CrossRef](#)]
30. Dash, D.; Kumar, S.; Mallika, C.; Kamachi Mudali, U. Temperature Dependency Studies on Volumetric Change and Structural Interaction in Aqueous Rare Earth Nitrate Solution. *J. Solut. Chem.* **2015**, *44*, 1812–1832. [[CrossRef](#)]
31. Jeon, J.H.; Yoon, C.G.; Ham, J.H.; Jung, K.W. Model development for nutrient loading estimates from paddy rice fields in Korea. *J. Environ. Sci. Health Part B Pestic. Food Contam. Agric. Wastes* **2004**, *39*, 845–860. [[CrossRef](#)]
32. Jyotiprava Dash, C.; Sarangi, A.; Singh, D.K.; Singh, A.K.; Adhikary, P.P. Prediction of root zone water and nitrogen balance in an irrigated rice field using a simulation model. *Paddy Water Environ.* **2015**, *13*, 281–290. [[CrossRef](#)]
33. Li, Y.; Šimůnek, J.; Jing, L.; Zhang, Z.; Ni, L. Evaluation of water movement and water losses in a direct-seeded-rice field experiment using Hydrus-1D. *Agric. Water Manag.* **2014**, *142*, 38–46. [[CrossRef](#)]
34. Patil, M.D.; Das, B.S. Assessing the effect of puddling on preferential flow processes through under bund area of lowland rice field. *Soil Tillage Res.* **2013**, *134*, 61–71. [[CrossRef](#)]

35. Phogat, V.; Yadav, A.K.; Malik, R.S.; Kumar, S.; Cox, J. Simulation of salt and water movement and estimation of water productivity of rice crop irrigated with saline water. *Paddy Water Environ.* **2010**, *8*, 333–346. [[CrossRef](#)]
36. Sutanto, S.J.; Wenninger, J.; Coenders-Gerrits, A.M.J.; Uhlenbrook, S. Partitioning of evaporation into transpiration, soil evaporation and interception: A comparison between isotope measurements and a HYDRUS-1D model. *Hydrol. Earth Syst. Sci.* **2012**, *16*, 2605–2616. [[CrossRef](#)]
37. Tan, X.; Shao, D.; Liu, H. Simulating soil water regime in lowland paddy fields under different water managements using HYDRUS-1D. *Agric. Water Manag.* **2014**, *132*, 69–78. [[CrossRef](#)]
38. Lee, M.S.; Lee, K.K.; Hyun, Y.; Clement, T.P.; Hamilton, D. Nitrogen transformation and transport modeling in groundwater aquifers. *Ecol. Model.* **2006**, *192*, 143–159. [[CrossRef](#)]
39. Gao, T.Z.; Fu, H.Y. Migration and transformation regularity of nitrogen in vadose zone in Hebei plain. *J. Saf. Environ.* **2015**, *15*, 217–221.
40. Jiang, G.H.; Wang, W.K. Numerical simulation and prediction of N transportation and transformation in unsaturated zone in Guanzhong Basin. *J. Northwest Univ.* **2007**, *95*, 825–829.
41. HJ/T166-2004; The Technical Specification for Soil Environmental Monitoring. China Environmental Science Press: Beijing, China, 2004.
42. HJ634-2012; Soil-Determination of Ammonium, Nitrite and Nitrate by Extraction with Potassium Chloride Solution-Spectrophotometric Methods. China Environmental Science Press: Beijing, China, 2012.
43. Yang, Y.R.; Tang, Z.H. Numerical simulation study on nitrate-nitrogen transportation and transformation in soil. *Yangtze River* **2019**, *50*, 53–57, (In Chinese with English abstract).
44. Pfannkuch, H. Contribution à l'étude des déplacements de fluides miscibles dans un milieu poreux [Contribution to the study of the displacement of miscible fluids in a porous medium]. *Rev. Inst. Fr. Pétr.* **1963**, *2*, 215–270.
45. Saiki, M.; Nguyen, T.P.M.; Shindo, J.; Nishida, K. Correction to: Nitrogen balance in paddy fields under flowing-irrigation condition. *Nutr. Cycl. Agroecosyst.* **2020**, *117*, 411. [[CrossRef](#)]
46. Feng, S.Y.; Zheng, Y.Q. Transformation and Loss of Nitrogen in Farmland and Its Impact on Aquatic Environment. *Agric. Environ. Prot.* **1996**, *6*, 277–279.
47. Yang, Q.H.; Zhang, H.T.; Hu, W.B.; Wang, H.J. Study on the Impact of Groundwater Level Changes on Nitrogen Export in the Middle Reaches of the Yangtze River. *J. Hydrogeol.* **2013**, *34*, 1–6.
48. Ma, Z.; Lian, X.; Jiang, Y.; Meng, F.; Xi, B.; Yang, Y.; Yuan, Z.; Xu, X. Nitrogen transport and transformation in the saturated-unsaturated zone under recharge, runoff, and discharge conditions. *Environ. Sci. Pollut. Res.* **2016**, *23*, 8741–8748. [[CrossRef](#)]
49. Sugita, F.; Nakane, K. Combined effects of rainfall patterns and porous media properties on nitrate leaching. *Vadose Zone J.* **2007**, *6*, 548–553. [[CrossRef](#)]
50. Gu, C.H.; William, J.R. Combined effects of short term rainfall patterns and soil texture on soil nitrogen cycling-A modeling analysis. *J. Contam. Hydrol.* **2010**, *112*, 141–154. [[CrossRef](#)]
51. Lazaratou, C.V.; Vayenas, D.V.; Papoulis, D. The role of clays, clay minerals and clay-based materials for nitrate removal from water systems: A review. *Appl. Clay Sci.* **2020**, *185*, 105377. [[CrossRef](#)]
52. Liu, J. *Study on Nitrogen Leaching Regulations on Three Textures of Soil*; Beijing Forestry University: Beijing, China, 2010.
53. Horn, R.; Taubner, H.; Wuttke, M.; Baumgartl, T. Soil physical properties related to soil structure. *Soil Tillage Res.* **1994**, *30*, 187–216. [[CrossRef](#)]
54. Jarvis, N.J. A review of non-equilibrium water flow and solute transport in soil macropores: Principles, controlling factors and consequences for water quality. *Eur. J. Soil Sci.* **2020**, *71*, 279–302. [[CrossRef](#)]
55. Bronswijk, J.J.B.; Hamminga, W.; Oostindie, K. Field-scale solute transport in a heavy clay soil. *Water Resour. Res.* **1995**, *31*, 517–526. [[CrossRef](#)]
56. Kurtzman, D.; Scanlon, B.R. Groundwater Recharge through Vertisols: Irrigated Cropland vs. Natural Land, Israel. *Vadose Zone J.* **2011**, *10*, 662–674. [[CrossRef](#)]
57. Sahile Gutema, S. Effects of Capillary Rise Saturation on Properties of Sub Grade Soil. *Am. J. Constr. Build. Mater.* **2021**, *5*, 32–49. [[CrossRef](#)]
58. Ben Neriah, A.; Assouline, S.; Shavit, U.; Weisbrod, N. Impact of ambient conditions on evaporation from porous media. *Water Resour. Res.* **2014**, *50*, 6696–6712. [[CrossRef](#)]

Disclaimer/Publisher's Note: The statements, opinions and data contained in all publications are solely those of the individual author(s) and contributor(s) and not of MDPI and/or the editor(s). MDPI and/or the editor(s) disclaim responsibility for any injury to people or property resulting from any ideas, methods, instructions or products referred to in the content.